DESIGN OF HALF-BAND DIAMOND AND FAN FILTERS BY SDP

T. Q. Hung, H. D. Tuan

Sch. of Elect. Eng. and Telecom., UNSW,
Sydney, NSW 2052, Australia
Email: hung.ta@student.unsw.edu.au, h.d.tuan@unsw.edu.au

T. Q. Nguyen

Dept. of Elect. and Comp. Eng., UCSD,
San Diego, CA 92093-0407, USA
Email: nguyent@ece.ucsd.edu

ABSTRACT

A new design method for linear phase half-band diamond (DS) and fan-shaped (FS) 2-D filters is proposed. A general formulation for frequency mask constraints in different shapes using 2-D trigonometric curves is developed. This facilitates semi-definite programming (SDP) of moderate dimension for the design problem. Several examples are included to illustrate advantages of our method.

Index Terms— Multidimensional digital filters, diamond filter, fan filter.

1. INTRODUCTION

Two-dimensional (2-D) filter and filter banks have been found in many applications of different fields (see e.g [1–7] and references therein). There are two types of filters: separable one as a product of two 1-D filters [2] and non-separable one [4–13]. Separable filters are easily designed but work mostly for rectangular spectrum division. Non-separable filters are preferred for other shapes of spectrum divisions such as diamond, fan etc. but their design is much more challenging [5, 9, 14]. The most important issues are: (i) the passband shape is accurately handled; (ii) the transition band is narrow enough; (iii) the peak-error in matching the ideal responses at the passband and stopband of the filter response is really small; (iv) the filter order is reasonable for efficient digital implementation. Nonseparable filters can still be designed from 1-D filters [8, 9, 15] with fast digital implementation but the shape of the filter passband is not easily controlled. The frequency sampling approach [14] can control the filter passband shape more efficiently but the transition band must be not so narrow to avoid singularity that may arise in interpolation. Recently, the semi-definite programming (SDP) has been applied to 2-D filter design [12, 13]. The SDP formulation allow filters to explicitly meet specific specifications without interpolation and thus is very flexible. However, unlike the 1-D case [16], the main issue there is that the dimension of SDP formulation may grow up explosively even for design of low-order filters. For instance, the dimension of each Gram matrix variable used in [12] is a high-order polynomial in filter-order. The masks for diamond-shaped filter have also been particularly considered in [12] but for academic purpose or ”theoretical results” rather than practical ones as emphasized in [12]. To avoid the curse of dimensionality arisen with the formulated SDPs, the diamond-shaped and fan-shaped passbands have been described just by unique first-order trigonometric polynomials (TPs) that are unlikely for accurate description. A much more delicate issue of practical design such as relation between frequency cutoff and coefficients of trigonometric polynomial for both passband and stopband description has not been addressed. It is also likely that the designed filters in [12] have a wide transition band. Some efficient SDP formulations of moderate dimension for rectangular passband and stopband filter have been proposed in [13]. The SDP dimension was also further reduced by using dual formulation. The designed filters in [13] also admit fast digital implementation though they are nonseparable and are not designed from 1-D filters. While the TPs for the exact description of a rectangle in frequency domain are almost obvious [13], they are not so easily derived for diamond shape and fan shape description. There are no TPs for their exact description and the TP description of moderate order for their accurate approximation is of great interest. The purpose of this paper is to provide such TP descriptions that lead to efficient SDP formulations for diamond shape and fan shape filters, i.e. those SDPs of moderate dimension that can be computed by existing SDP software. The richness and efficiency of the proposed class of SDP formulations are clearly articulated by the fact that compared with those designed by other existing methodologies such as frequency sampling [14], our designed filters have narrower transition bands, better both the passband ripple and stopband attenuation while admitting a fast implementation (i.e. they are of low complexity).

The paper is organized as follows. Section 2 is devoted to a general strategy and SDP formulation for the 2-D filter design. They are concretized in Section 3 and Section 4 for designing diamond and fan filters, respectively. Finally, Section 4 gives some concluding remarks.

The notations used in this paper are rather standard, except that $\langle \mathbf{A} \rangle$ refers to the trace of a square matrix $\mathbf{A}$, so $\langle \mathbf{AB} \rangle = \langle \mathbf{BA} \rangle$ for any matrices $\mathbf{A}$ and $\mathbf{B}$. By $\mathbf{X} \geqslant 0$ ($\mathbf{X} > 0$) we mean a symmetric positive (strictly positive) definite matrix

$\mathbf{X}$. One of the main property of positive definite matrices that will be often used in the paper is $\langle \mathbf{XY} \rangle \geqslant 0$ whenever $\mathbf{X} \geqslant 0$ and $\mathbf{Y} \geqslant 0$. By TPs, in this paper we refer to that involving the trigonometric powers $\cos(i\omega_1)\cos(j\omega_2)$.

2. GENERAL SDP FORMULATION

The paper focuses on the following frequency response of a zero-phase four-fold filter $\mathcal{H}(z_1, z_2)$

$$H(\Omega) = \boldsymbol{\varphi}_n^T(\omega_1)\mathbf{X}\boldsymbol{\varphi}_n(\omega_2) = \langle \mathbf{X}, \mathbf{M}(\Omega) \rangle, \tag{1}$$

where

$$\Omega := (\omega_1, \omega_2), \in [0, \pi]^2, \; \mathbf{X} = [x_{i\ell}]_{i,\ell=0}^n,$$
$$\boldsymbol{\varphi}_n(\omega_i) = (1, \cos\omega_i, \cos 2\omega_i, \ldots, \cos n\omega_i)^T,$$
$$\mathbf{M}(\Omega) = \boldsymbol{\varphi}_n(\omega_1)\boldsymbol{\varphi}_n^T(\omega_2).$$

The design of the filter $\mathcal{H}(z_1, z_2)$ involves a solution of the matrix $\mathbf{X}$ of filter coefficients such that the frequency response $\mathcal{H}(\Omega)$ satisfies a given set of specifications and the following optimization based design can be formulated

$$\min_{\mathbf{X}} \quad \sum_{i=1}^{L} \langle \mathbf{M}_{1i}\mathbf{X}\mathbf{M}_{2i}\mathbf{X}^T \rangle - \langle \mathbf{MX} \rangle \tag{2}$$

$$\text{s.t.} \quad -\delta_p \leqslant \langle \mathbf{XM}(\Omega) \rangle - 1 \leqslant \delta_p \qquad \forall \Omega \in \Omega_p \tag{3}$$

$$-\delta_s \leqslant \langle \mathbf{XM}(\Omega) \rangle \leqslant \delta_s \qquad \forall \Omega \in \Omega_s \tag{4}$$

with some predefined matrices $\mathbf{M}_{1i} > 0, \mathbf{M}_{2i} > 0$ and $\mathbf{M}$. Here the quadratic objective (2) is an approximation of the minimal weighted-square error $W_p \int_{\Omega_p} |H(\Omega) - 1|^2 d\Omega + W_s \int_{\Omega_s} |H(\Omega)|^2 d\Omega$, $d\Omega = d\omega_1 d\omega_2$, $W_p > 0$, $W_s > 0$, while the semi-infinite constraints (3)-(4) are the peak-error constrained $|H(\Omega) - 1| \leqslant \delta_p$, $\forall \Omega \in \Omega_p$ on passband and $|H(\Omega)| \leqslant \delta_s$, $\forall \Omega \in \Omega_s$ in stopband.

Like [13] we aim at deriving effective SDP formulations for SI constraints (3)-(4), which accurately reflect the shapes of the passband and stopband while not result on highly dimensional SDPs. We now provide our strategy to resolve these two issues.

First, each region Ω_I ($I \in \{p, s\}$) is described by TPs of the first order

$$\mathcal{T}_{1i}^{(I)}(\Omega) - b_i^{(I)} \quad \geqslant \quad 0; \;\; i = 1, 2, \ldots, M_I. \tag{5}$$

Define Chebysev recursions

$$T_{0i}^{(I)}(\Omega) = 1, \; T_{1i}^{(I)}(\Omega) = \mathcal{T}_{1i}^{(I)}(\Omega) - b_i^{(I)};$$
$$T_{ji}^{(I)}(\Omega) = 2T_{(j-1)i}^{(I)}(\Omega)T_{1i}^{(I)}(\Omega) - T_{(j-2)i}^{(I)}(\Omega), \; j = 2, 3, \ldots \tag{6}$$

Then, for $m = [(n-1)/2]$, the moment matrices are constructed as

$$\boldsymbol{\Psi}_i^{(I)}(\Omega) = \begin{bmatrix} 1 \\ T_{1i}^{(I)}(\Omega) \\ \ldots. \\ T_{mi}^{(I)}(\Omega) \end{bmatrix} \begin{bmatrix} 1 \\ T_{1i}^{(I)}(\Omega) \\ \ldots. \\ T_{mi}^{(I)}(\Omega) \end{bmatrix}^T. \tag{7}$$

Further, with the definitions

$$\boldsymbol{\Theta}_i(\Omega) \quad = \quad (\mathcal{T}_{1i}^{(I)}(\Omega) - b_i)\boldsymbol{\Psi}_i(\Omega) \tag{8}$$

and

$$\mathcal{C}_I = \quad \{\mathbf{X} \in R^{(n+1)\times(n+1)} : \quad \langle \mathbf{XM}(\Omega) \rangle \equiv \sum_{i=1}^{M_I} \langle \mathbf{X}_i, \boldsymbol{\Theta}_i(\Omega) \rangle,$$
$$\mathbf{X}_i \geqslant 0, \boldsymbol{\Psi}_i(\Omega) \geqslant 0\}, \tag{9}$$

we then effective strengthen SIP (2)-(4) by the following SDP

$$\min_{\mathbf{X}}(2) : \quad \mathbf{X} - (1 - \delta_p)\mathbf{E}_1 \in C_p, \; -\mathbf{X} + (1 + \delta_p)\mathbf{E}_1 \in C_p$$
$$\mathbf{X} + \delta_s\mathbf{E}_1 \in C_s, \; -\mathbf{X} + \delta_s\mathbf{E}_1 \in C_s \tag{10}$$

where $\mathbf{E}_1 \in R^{(n+1)\times(n+1)}$ with zero entries except $\mathbf{E}_1(0,0) = 1$. It can be shown that SDP constraints (10) imply SI constraints (3)-(4). It should be emphasized that the effectiveness of SDP (10) is confirmed by simulations in the next sections with designing of diamond and fan filters with narrow transition band. Moreover, due the representation (9) for the filter coefficient matrix $= \mathbf{X}$ they admit a fast implementation as well.

The dual cone $\mathcal{C}_I^* = \{\mathbf{Y} : \langle \mathbf{YX} \rangle \geqslant 0, \forall \mathbf{X} \in \mathcal{C}_\alpha\}$ is described by SDP constraint

$$\mathcal{C}_I^* = \{\mathbf{Y} \in R^{(n+1)\times(n+1)} : \; \boldsymbol{\Theta}_i(\mathbf{Y}) \geqslant 0, \; \boldsymbol{\Psi}_i(\mathbf{Y}) \geqslant 0; \; i = 1, \ldots, M_I\} \tag{11}$$

where $\boldsymbol{\Theta}_i(\mathbf{Y})$ and $\boldsymbol{\Psi}_i(\mathbf{Y})$ are created from $\boldsymbol{\Theta}_i(\Omega)$ and $\boldsymbol{\Psi}_i(\Omega)$ by the variable change

$$y_{j\ell} \leftarrow \cos(j\omega_1)\cos(\ell\omega_2), \; j, \ell = 0, 1, 2, \ldots, n.$$

So the optimal solution $\mathbf{X}_{opt}$ of (10) is found from the dual SDP is

$$\max_{\mathbf{Y}^{(i)}, \mathbf{X}_{opt}} \; [\langle(((1 - \delta_p)\mathbf{Y}^{(1)} - (1 - \delta_p)\mathbf{Y}^{(2)} - \delta_s(\mathbf{Y}^{(3)}$$
$$+\mathbf{Y}^{(4)}))\mathbf{E}_1\rangle - \sum_{i=1}^{L} \langle \mathbf{M}_{1i}\mathbf{X}_{opt}\mathbf{M}_{2i}\mathbf{X}_{opt}^T \rangle] \; :$$
$$\mathbf{Y}^{(1)} \in C_p^*, \; \mathbf{Y}^{(2)} \in C_p^*, \; \mathbf{Y}^{(3)} \in C_s^*, \; \mathbf{Y}^{(4)} \in C_s^*,$$
$$2\sum_{i=1}^{L} \mathbf{M}_{2i}\mathbf{X}_{opt}^T\mathbf{M}_{1i} - \mathbf{M} - \mathbf{Y}^{(1)} + \mathbf{Y}^{(2)} - \mathbf{Y}^{(3)} + \mathbf{Y}^{(4)} = 0 \tag{12}$$

3. HALF-BAND DIAMOND FILTER DESIGN

The diamond filter (DF) with cutoff frequency at $\pi/2$ is also known as a half-band 2-D filter.

Figure 1 depicts the passband (dotted) and the stopband (white) of the ideal half-band DF (part (a)) and our designed DF (part (b)). The cutoff frequency of the ideal passband and the stopband is $(\omega_{1c}, \omega_{2c}) =$

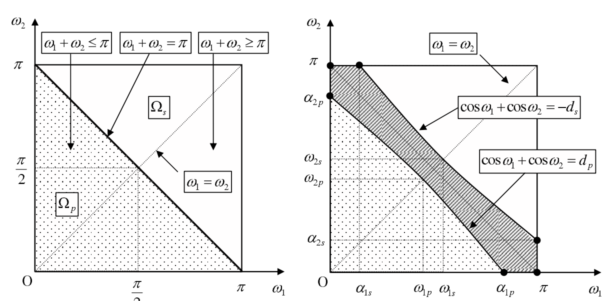

(a) Ideal half-band filter (b) Relaxation of passband and stopband

Fig. 1. Diamond four-fold filter

$(\pi/2, \pi/2)$. In practical design, there must be a transition band between them. For the cutoff frequencies $(\omega_{1p}, \omega_{2p}), \omega_{1p} = \omega_{2p} \leqslant$

Table 1. Performance comparison for DS filter

Specifications	Our method	NDFT method
δ_p	0.017	0.0189
δ_s	0.015	0.0184
ω_{1p}	0.43π	0.36π
ω_{1s}	0.67π	0.64π

$\pi/2$ for the passband and $(\omega_{1s}, \omega_{2s}), \omega_{1p} < \omega_{1s} = \omega_{2s} \geqslant \pi/2$ have been chosen. The width of the transition band is characterized by the difference $\omega_{1s} - \omega_{1p}$ between passband and stopband cutoff frequencies.

Then diamond-shaped (DS) passband is approximately described by

$$\begin{array}{l} \cos\omega_1 + \cos\omega_2 \geqslant d_p;\ d_p = 2\cos\omega_{1p}, \\ \alpha_{1p} \geqslant \omega_1 \geqslant 0,\ \alpha_{1p} = \mathsf{arccos}(d_p - 1); \\ \alpha_{2p} \geqslant \omega_2 \geqslant 0,\ \alpha_{2p} = \mathsf{arccos}(d_p - 1), \end{array} \tag{13}$$

while the stopband is approximately described by

$$\begin{array}{l} \cos\omega_1 + \cos\omega_2 \leqslant -d_s;\ d_s = -2\cos\omega_{1s}, \\ \alpha_{1s} \leqslant \omega_1 \leqslant \pi,\ \alpha_{1s} = \mathsf{arccos}(1 - d_s), \\ \alpha_{2s} \leqslant \omega_2 \leqslant \pi,\ \alpha_{2s} = \mathsf{arccos}(1 - d_s) \end{array} \tag{14}$$

Note that the choice $\omega_{1p} = \pi/2$ ($\omega_{1s} = \pi/2$, resp.) will make (13) ((14), resp.) the exact description for the ideal passband (stopband, resp.).

Therefore, we can write

$$\begin{array}{ll} \Omega_p \approx & \{(\omega_1, \omega_2) : \cos\omega_1 + \cos\omega_2 \geqslant d_p, \\ & \cos\omega_1 \geqslant d_p - 1,\ \cos\omega_2 \geqslant d_p - 1\} \\ \Omega_s \approx & \{\cos\omega_1 + \cos\omega_2 \leqslant -d_s, \\ & \cos\omega_1 \leqslant 1 - d_s, \cos\omega_2 \leqslant 1 - d_s\}. \end{array}$$

and the first order polynomials $\mathcal{T}_{1i}^{(I)}$ and constants $b_i^{(I)}$ for (5) are concretized for this cases as following

$$\begin{array}{lcl} \mathcal{T}_{11}^{(p)} - b_1^{(p)} & = & \cos\omega_1 + \cos\omega_2 - d_p, \\ \mathcal{T}_{12}^{(p)} - b_2^{(p)} & = & \cos\omega_1 + \cos\omega_2 + 2 - 2d_p, \\ \mathcal{T}_{13}^{(p)} - b_3^{(p)} & = & (\cos\omega_1 + 1 - d_p)(\cos\omega_2 + 1 - d_p); \\ \mathcal{T}_{11}^{(s)} - b_1^{(s)} & = & -\cos\omega_1 - \cos\omega_2 - d_s, \\ \mathcal{T}_{12}^{(s)} - b_2^{(s)} & = & -\cos\omega_1 - \cos\omega_2 + 2 - 2d_s, \\ \mathcal{T}_{13}^{(s)} - b_3^{(s)} & = & (-\cos\omega_1 + 1 - d_s)(-\cos\omega_2 + 1 - d_s) \end{array}$$

Figure 2 depicts the frequency response of the designed DF with size 19×19 with designed parameters given by Table 1. A comparison of our result and that by the nonuniform discrete Fourier transform (NDFT) [14] can be also revealed from this table: our filter is better in term of small ripples over supported regions and narrow transition band while is of much lower complexity (as mentioned in the previous sections)

4. FAN FILTER DESIGN

The fan filter (FF) is a special filter with directional sensitivity. Therefore, FF can be used in many applications such as geoseismic data processing. Although its shape is different from the diamond, the fan shape masks can be similarly handled. Figure 3 depicts the passband (dotted) and the stopband (white) of the ideal FF and that designed

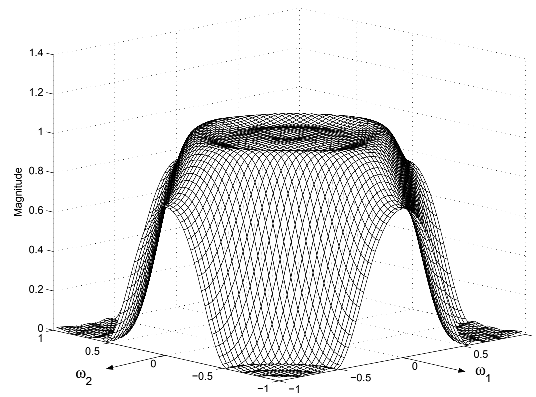

Fig. 2. Frequency response of the designed DF

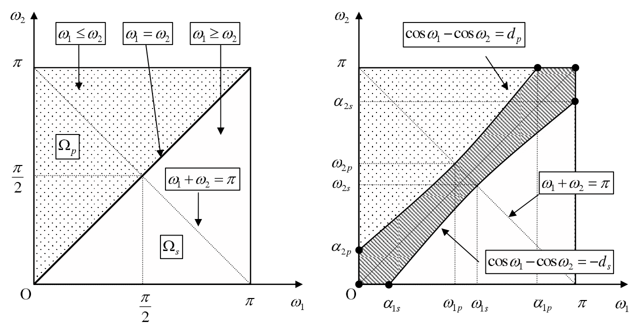

(a) Ideal fan-shaped filter

(b) Relaxation of passband and stopband

Fig. 3. Fan four-fold filter

by our method. The cutoff frequency for the ideal passband and stopband is $(\omega_{1c}, \omega_{2c}) = \pi/2$. With a choice of passband cutoff frequency $(\omega_{1p}, \omega_{2p}), \pi/2 \geqslant \omega_{1p} = \pi - \omega_{2p}$ and stopband cutoff frequency $(\omega_{1s}, \omega_{2s}), \pi/2 \leqslant \omega_{1s} = \pi - \omega_{2s} > \omega_{1p}$, the passband is approximately described by

$$\begin{array}{l} \cos\omega_1 - \cos\omega_2 \geqslant d_p,\ d_p = 2\cos(\omega_{1p}), \\ \alpha_{1p} \geqslant \omega_1 \geqslant 0,\ \alpha_{1p} = \mathsf{arccos}(d_p - 1), \\ \pi \geqslant \omega_2 \geqslant \alpha_{2p},\ \alpha_{2p} = \mathsf{arccos}(1 - d_p) \end{array} \tag{15}$$

while the stopband is approximately described by

$$\begin{array}{l} \cos\omega_1 - \cos\omega_2 \leqslant -d_s,\ d_s = -2\cos(\omega_{1s}), \\ \pi \geqslant \omega_1 \geqslant \alpha_{1s},\ \alpha_{1s} = \mathsf{arccos}(d_s - 1), \\ \alpha_{2s} \geqslant \omega_2 \geqslant 0, \alpha_{2s} = \mathsf{arccos}(1 - d_s). \end{array} \tag{16}$$

Again, the width of the transition band is characterized by the difference $\omega_{1s} - \omega_{1p}$ and the choice $\omega_{1p} = \pi/2$ ($\omega_{1s} = \pi/2$, resp.) will make (15) ((16), resp.) the exact description for the ideal passband (stopband, resp.).

The first order polynomials $\mathcal{T}_{1i}^{(I)}$ and constants $b_i^{(I)}$ for (5) are con-

Table 2. Performance comparison for FF

Specifications	Our method	NDFT method
δ_p	0.005	0.0051
δ_s	0.0025	0.0051
ω_{1p}	0.42π	0.43π
ω_{1s}	0.65π	0.57π

cretized for this cases as following

$$\begin{aligned}
\mathcal{T}_{11}^{(p)} - b_1^{(p)} &= \cos\omega_1 - \cos\omega_2 - d_p, \\
\mathcal{T}_{12}^{(p)} - b_2^{(p)} &= \cos\omega_1 - \cos\omega_2 + 2 - 2d_p, \\
\mathcal{T}_{13}^{(p)} - b_3^{(p)} &= (\cos\omega_1 + 1 - d_p)(-\cos\omega_2 + 1 - d_p); \\
\mathcal{T}_{11}^{(s)} - b_1^{(s)} &= -\cos\omega_1 + \cos\omega_2 - d_s, \\
\mathcal{T}_{12}^{(s)} - b_2^{(s)} &= -\cos\omega_1 + \cos\omega_2 + 2 - 2d_s, \\
\mathcal{T}_{13}^{(s)} - b_3^{(s)} &= (-\cos\omega_1 + 1 - d_s)(\cos\omega_2 + 1 - d_s)
\end{aligned}$$

Figure 4 depicts the frequency response of the FF with size 19×19. The specification parameters are given by table 2. As can be seen, the ripples of passband and stopband are still very small, particularly showing the efficiency of our method. As mentioned in Sections 1 and 2, our designed filter is of much lower complexity than that of the same order designed by the frequency sampling one.

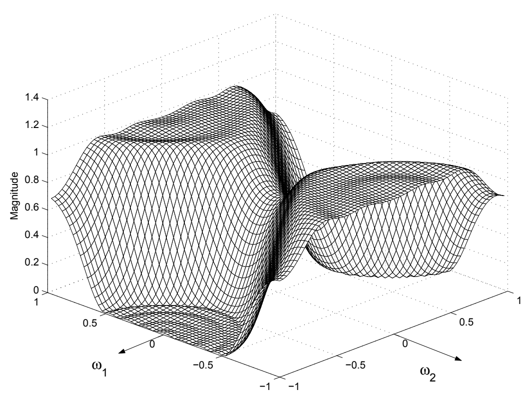

Fig. 4. Frequency response of the designed FF

5. CONCLUSION

This paper has discussed a general technique for the design of half-band DF and FF with frequency mask constraints. The most advantage of this technique is that filters are designed based on SDPs of moderate size. The frequency mask specifications of diamond-shaped and fan-shaped are assured in our setting. Numerical results have manifested the viability of our approach and its advantages over existing methods.

6. REFERENCES

[1] T. Chen and P. P. Vaidyanathan, "Multidimensional multirate filters and filter banks derived from one-dimensional filters," *IEEE Transaction on Signal Processing*, vol. 41, no. 5, pp. 1749–1765, May 1993.

[2] T. Chen and P. P. Vaidyanathan, "Recent development in multidimensional multirate systems," *IEEE Transaction on Circuits and Systems for Video Technology*, vol. 3, no. 2, pp. 116–137, April 1993.

[3] J. S. Geromino and H. J. Woerdeman, "Positive extensions, Fejer-Riesz factorization and autoregressive filters in two variables," *Annals of Mathematics*, vol. 160, no. 3, pp. 839–906, 2004.

[4] J. S. Lim, *Two-dimensional signal and image processing*, Prentice-Hall, Englewood Cliffs, NJ, USA, 1990.

[5] K. S. C. Pun and T. Q. Nguyen, "A novel and efficient design of multidimensional PR two-channel filter banks with hourglass-shaped passband support," *IEEE Signal Processing Letters*, vol. 11, no. 3, pp. 345–348, March 2004.

[6] J. Zhou, M. N. Do, and J. Kovacevic, "Multidimensional orthogonal filter bank characterization and design using the Calys transform," *IEEE Transaction on Image Processing*, vol. 14, no. 6, pp. 760–769, June 2005.

[7] J. W. Woods, *Multidimensional Signal, Image, and Video Processing and Coding*, Elsevier Inc., Burlington, MA, USA, 2006.

[8] J. H. McClelan, "The design of two-dimensional digital filters by tranformations," in *Proceeding 7th Annual Princeton Conference Information Sciences and Systems*, 1973, pp. 247–251.

[9] R. M. Merserreau, W. F. G. Mecklenbräuker, and T. F. Quatieri, "McClellan transformation for two-dimensional digital filtering: I-design," *IEEE Transaction on Circuits and Sytems*, vol. 23, no. 7, pp. 405–414, July 1976.

[10] W. S. Lu and A. Antoniou, *Two-Dimensional Digital Filters*, Marcel Dekker Inc., New York, NY 10016, USA, 1992.

[11] W. S. Lu and T. Hinamoto, "Optimal design of frequency-response-masking filters using semidefinite programming," *IEEE Transactions on Circuits and Systems-I: Fundamental Theory and Applications*, vol. 50, no. 4, pp. 557–568, April 2003.

[12] B. Dumitrescu, "Design of 2-D FIR filters using positive trigonometric polynomials," in *International Conference on Acoustic, Speech and Signal Processing (ICASSP)*, Toulouse, May 2006, IEEE, pp. 512–515.

[13] T. Q. Hung, H. D. Tuan, B. Vo, and T. Q. Nguyen, "SDP for 2-D filter design: General formulation and dimension reduction techniques," in *International Conference on Acoustic, Speech and Signal Processing (ICASSP)*, Toulouse, May 2006, IEEE, pp. 621–624.

[14] S. Bagchi and S. K. Mitra, "The nonuniform discrete fourier transform and its applications in filter design: Part II-2-D," *IEEE Trans. Circuits and Systems-II: Analog and Digital Signal Processing*, vol. 43, no. 6, pp. 434–444, June 1996.

[15] C. K. Chen and J. H. Lee, "McClellan transform based design techniques for two-dimensional linear-phase FIR filters," *IEEE Transaction on Circuits and Systems -I: Fundamental Theory and Applications*, vol. 41, no. 8, pp. 505–517, August 1994.

[16] H. D. Tuan, T. T. Son, B. Vo, and T. Q. Nguyen, "LMI characterization for the convex hull of trigonometric curves and applications," in *International Conference on Acoustic, Speech and Signal Processing (ICASSP)*, Philadelphia, March 2005, IEEE, pp. 425–428.